Ocean Engineering 305 (2024) 117957

Contents lists available at ScienceDirect

Ocean Engineering

journal homepage: www.elsevier.com/locate/oceaneng

Route, speed, and bunkering optimization for LNG-fueled tramp ship with alternative bunkering ports

Ping He [a], Jian Gang Jin [a,b,*], Wei Pan [c], Jianghang Chen [d]

[a] School of Ocean and Civil Engineering, and MOE Key Laboratory of Marine Intelligent Equipment and System, Shanghai Jiao Tong University, Shanghai 200240, China
[b] State Key Laboratory of Ocean Engineering, Shanghai Jiao Tong University, Shanghai 200240, China
[c] Institute for Big Data Research, Liaoning University of International Business and Economics, Dalian 116052, China
[d] International Business School, Xi'an Jiaotong-Liverpool University, Suzhou 215123, China

ARTICLE INFO

Keywords:
LNG-fueled tramp ship
Alternative bunkering ports
Optimization of shipping line
Mixed-integer programming

ABSTRACT

To reduce emissions, shipping companies are deploying eco-friendly ships, like those powered by LNG or methanol. Unlike traditional fuels, LNG bunkering is available at a limited number of ports. At the same time, tramp or bulk ships have fewer ports of call on their shipping lines, which may necessitate LNG-fueled ships sailing to alternative bunkering ports for refueling. The selection of bunkering ports impacts the operating costs of shipping lines due to differences in fuel prices and geographical locations. Moreover, it must factor in ship speed limits to meet loading and unloading schedules. To optimize the shipping route, speeds, and bunkering plan for LNG-fueled tramp ships, we develop an arc-based mixed-integer linear programming model with the objective of minimizing total operation costs. Subsequently, we propose a leg-based formulation based on the predetermined port call orders. Finally, case studies are conducted to demonstrate the effectiveness and efficiency of the models. Experimental results indicate that the bunkering mode with alternative bunkering ports effectively reduces total operating costs without altering the total voyage time, particularly with substantial differences in fuel prices between ports.

1. Introduction

The advantages of maritime transport, such as high transportation volume and low cost, establish its indispensable role in global merchandise transportation, with approximately 80 percent of cargo worldwide transported by sea (Wei et al., 2022). Nevertheless, the shipping industry is currently under pressure to reduce greenhouse gas (GHG) emissions (Taskar et al., 2023). Traditional marine fuels, like Heavy Fuel Oil (HFO), serve as the primary power source for ships, yet they generate substantial quantities of greenhouse gases. In 2022, the shipping industry emitted a total of 706 million tonnes of CO2, accounting for two percent of global CO2 emissions (International Energy Agency). In response to these environmental concerns, the International Maritime Organization (IMO) introduced a series of policy measures. For instance, the 2023 IMO Revised GHG Strategy (IMO) mandates a 40% reduction in carbon emissions from the shipping industry by 2030, compared to 2008. To comply with these policy requirements, shipping companies are transitioning to cleaner fuels such as LNG and methanol. Consequently, an increasing number of shipping companies are deploying ships fueled by LNG or methanol. As of December 2023, 411 LNG-fueled ships are in operation, with an additional 526 LNG-fueled ships on order (SEA LNG).

At present, the majority of ports cannot bunker LNG fuels, necessitating ships, particularly tramp ships, to seek refueling services at alternative ports apart from designated loading or unloading ports. Unlike liner shipping routes, tramp shipping lines typically involve only several loading and unloading ports. Additionally, ports available for LNG bunkering are primarily concentrated in Europe and the east coast of the United States, with limited availability in other regions such as Asia and Australia, as depicted in Fig. 1 . Consequently, tramp ships unable to refuel at their designated loading or unloading ports are compelled to call other ports for bunkering. For instance, the tramp ship following the route of Jingtang–Qinzhou–Hedland–San Antonio (CL), as shown in Fig. 1, may bunker LNG at alternative ports like Shanghai, Ningbo, Shenzhen, Singapore, or Dampier.

Bunker prices exhibit significant variations among ports, providing shipping companies with an opportunity to reduce bunker costs by selecting bunkering ports with lower fuel prices (Zhen et al., 2017). Fig. 2 shows prices of the very low-sulfur fuel oil (VLSFO) at major bunkering ports worldwide on December 24, 2023. Given that fuel costs

* Corresponding author.
E-mail address: jiangang.jin@sjtu.edu.cn (J.G. Jin).

https://doi.org/10.1016/j.oceaneng.2024.117957
Received 17 January 2024; Received in revised form 15 April 2024; Accepted 19 April 2024
Available online 2 May 2024

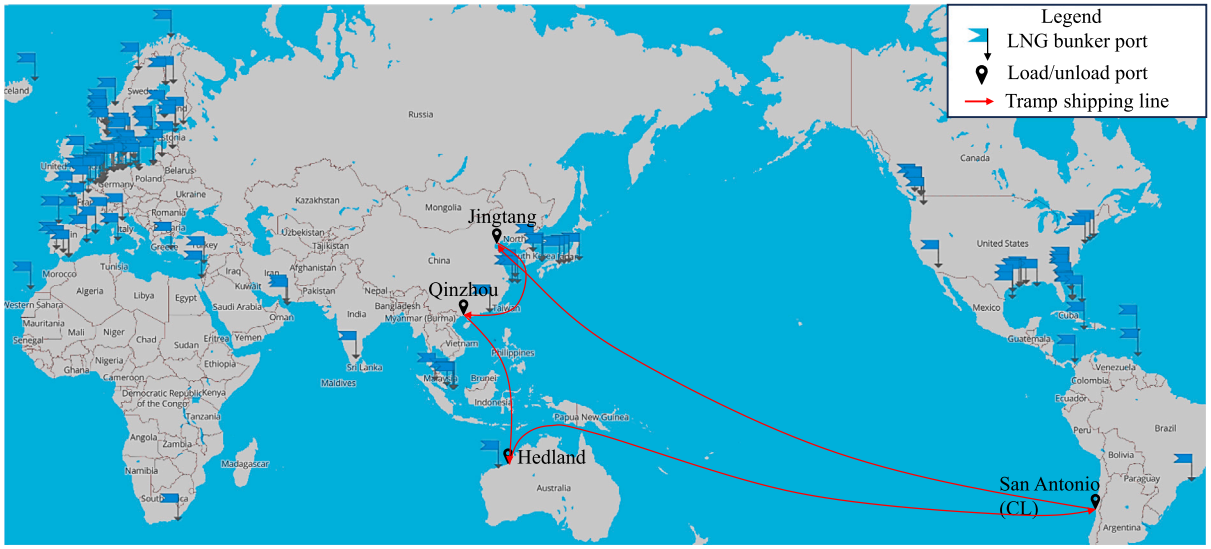

Fig. 1. LNG bunker ports worldwide and a tramp shipping line.
Source: (SEA LNG).

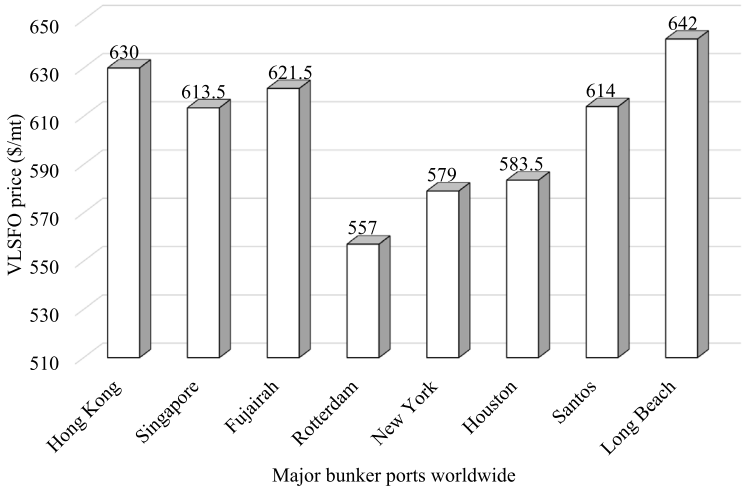

Fig. 2. VLSFO bunker prices at major bunker ports worldwide on 24/12/2023.
Source: (Ship&Bunker).

constitute more than 50% of the total voyage expenses (Meng et al., 2015), this strategy can effectively slash the operating costs of shipping lines, and thus increase the profitability of shipping lines.

Due to the different geographical locations of alternative bunker ports, bunkering at different ports will result in varying increases in total sailing distances. To ensure that the schedule for visiting loading and unloading ports remains unaffected by the detour, consideration of the vessel's speed limit becomes crucial when selecting the refueling port. Additionally, sailing speeds impact fuel consumption, with higher speeds leading to increased fuel consumption, thus impacting the bunker plan. Therefore, for the operation of a shipping line with an LNG-fueled ship, shipping companies need to comprehensively consider interrelated factors such as voyage speed, bunker port, and bunker volume to minimize operating costs while meeting constraints like the latest time for port calls. This introduces new decision-making challenges to the operation of tramp shipping lines.

Fig. 3 provides an intuitive demonstration of the differences in routes, speeds, and the choice of bunker ports between conventional and LNG-fueled ships when transporting two batches of cargo. Fig. 3(a) shows the route of a conventional tramp ship that can bunker at any loading or unloading port. Operating such a conventional tramp shipping line only necessitates consideration of sailing speeds on each leg and the bunker volume on each loading or unloading port. As these ports are unable to bunker LNG, the LNG-fueled ship must deviate from this route to alternative ports for bunkering. Figs. 3(b) and 3(c) show two routes for transporting these cargoes with an LNG-fueled ship. In Fig. 3(b), the ship bunkers at port 1, whereas in Fig. 3(c), it bunkers at port 2. Both routes 1 and 2 require detours to accommodate the call of bunker ports. To guarantee timely arrivals at loading and unloading ports, the ship may speed up during its journey to the refueling port and subsequent ports, as shown in Figs. 3(b) and 3(c).

To address the challenges associated with optimizing the sailing route, speeds, and bunkering for LNG-fueled tramp ships, we first formulate an arc-based mixed-integer linear programming (MILP) model. This model aims to minimize overall operating costs, encompassing fuel costs and the ship's daily operating costs. Moreover, it incorporates critical factors such as ensuring a safe fuel volume, adhering to port call schedules, and considering fuel consumption at different speeds in laden and ballast conditions. Subsequently, we develop a highly efficient leg-based model, leveraging the predetermined sequence of port calls. Finally, we validate the effectiveness of models through numerical experiments and conduct a comprehensive analysis comparing the total

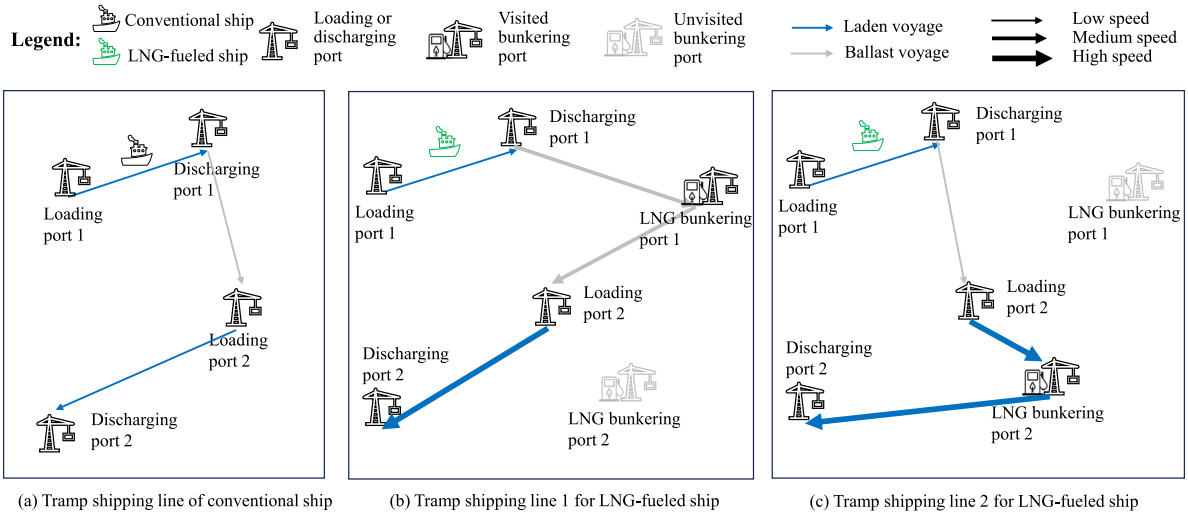

Fig. 3. An illustrative example of the differences between the traditional tramp shipping line and the shipping line of LNG-fueled ships.

operation costs, fuel consumption, and bunker strategies between the conventional and LNG-fueled tramp shipping lines.

Our contributions in this paper are summarized as follows:

(1) We introduce an optimization problem for the tramp shipping line utilizing the LNG-fueled ship. This problem encompasses factors inherent in the operation of traditional tramp shipping lines, including sailing speeds at different legs and refueling volume at loading and unloading ports. Additionally, it tackles the necessity to bunker at alternative bunkering ports, requiring corresponding adjustments of speeds and routes.

(2) We develop arc-based and leg-based mixed-integer linear programming models. Notably, the leg-based model exhibits superior computational performance, capable of finding optimal solutions for real-scale problems within two seconds.

(3) We demonstrate, through case studies, that refueling at optimal bunker ports selected from LNG-bunkering available loading, unloading, and other alternative bunker ports not only has no impact on the voyage time but also reduces operation costs. This is particularly evident in scenarios with significant fuel price fluctuations across different ports.

The remainder of this study is organized as follows. Section 2 reviews related work and positions our work. Section 3 elaborates on the investigated joint optimization problem and introduces two mathematical models. Case studies are conducted in Section 4. Conclusions and future work are presented in Section 5.

2. Literature review

In this section, we review two streams of literature closely related to our study: (1) alternative fuels in the shipping industry; and (2) optimization of routes, speed, and bunkering for shipping lines.

2.1. Alternative fuels in shipping industry

At the policy level, international organizations like the European Union (EU) have introduced a range of policies and measures to encourage the adoption of cleaner alternative fuels within the shipping industry. As early as 2009, the EU implemented the European Energy Taxation Directive (ETD), which focused on promoting the use of renewable energy and enhancing energy efficiency through taxation (European Commission). Additionally, the EU enacted the Renewable Energy Directive (RED) in the same year, which established targets for the proportion of renewable energy in overall energy consumption. Member countries are obligated to take measures to promote the development and utilization of renewable energy. To further promote cleaner energy adoption, the EU revised the RED and issued RED II in 2018. The revision aims for renewable energy to constitute a minimum of 32% of final energy consumption by 2030 (European Commission). In 2021, the EU proposed the 'Fit for 55' emissions reduction program (European Council), which seeks to achieve a minimum of 55% reduction in the EU's net GHG emissions by 2030 compared to 1990, with the ultimate goal of climate neutrality by 2050. To achieve this, 'Fit for 55' proposes a set of specific policy measures. The FuelEU Maritime Directive, a component of 'Fit for 55', targets renewable and low-carbon fuels (RLF) constituting 86%–88% of the fuel mix for international maritime transportation by 2050 (DNV).

Numerous studies have explored the emission reduction potential of alternative fuels. Hansson et al. (2019) employed multi-criteria decision analysis to evaluate seven alternative fuels for the shipping industry. Evaluation results ranked LNG as the most promising alternative fuel, followed by HFO (Heavy Fuel Oil), methanol, and bio-fuels. Deniz and Zincir (2016) compared four alternative fuels, including methanol, ethanol, LNG, and hydrogen. They concluded that LNG is the most suitable alternative marine fuel, followed by hydrogen. Ren and Liang (2017) concluded that hydrogen is the most sustainable fuel, with LNG following closely behind. Balcombe et al. (2021) conducted a comprehensive environmental and cost assessment of LNG, with results demonstrating that LNG can reduce GHG emissions by up to 28% compared to HFO. Lindstad et al. (2022) investigated the potential reductions for GHG emissions by combining ship design and alternative fuels. Bayraktar and Yuksel (2023) examined the EEXI (Energy Efficiency Existing Ship Index) values and CII (Carbon Intensity Indicator) ratings of five types of ships with different main engine configurations, concluding that alternative fuels such as LNG, with a low carbon factor and a higher calorific value, can significantly reduce EEXI and CII ratings.

2.2. Optimization of route, speed, and bunkering for shipping lines

A considerable number of studies have focused on optimizing routes, speeds, and bunkering to reduce fuel consumption, minimize operating costs, or maximize total revenue for shipping companies. For instance, Fagerholt et al. (2010) developed a non-linear programming model to reduce fuel consumption by optimizing the speed of a tramp shipping route. Norstad et al. (2011) investigated a tramp ship routing and scheduling problem with speed optimization to maximize total revenue and developed a local search algorithm to solve it. Meng et al. (2015) explored a joint optimization problem of tramp ship routing and bunkering to maximize total profits and proposed a branch-and-price algorithm for obtaining the exact solution. Zhen et al. (2017)

designed a dynamic programming algorithm to obtain optimal ship bunkering decisions while considering stochastic fuel consumption in each leg and stochastic bunkering prices. Zhen et al. (2020) proposed a mixed integer linear programming formulation to optimize speeds and routes considering the Emission Control Areas (ECAs) policy, with the objective of minimizing total fuel cost and emissions. Wang et al. (2020) proposed a joint optimization model of sailing routes and speeds to mitigate ship energy consumption and CO2 emissions. Numerical experiments demonstrated a reduction by approximately 4%. Wei et al. (2022) established a mathematical formulation to minimize fuel consumption by optimizing ship route and sailing speed, developing a heuristic algorithm to solve the problem. Taskar et al. (2023) introduced a methodology to optimize ship speed without altering the shipping route and observed up to 6% fuel savings through case studies. Mason et al. (2023a) developed a wind propulsion and voyage optimization model to quantify the potential of reducing CO2 emissions and demonstrated that it is possible to cut 60% of CO2. Mason et al. (2023b) investigated the fuel consumption of shipping routes considering stochastic uncertainty arising from wind forecasts. Their findings indicated that routes with favorable wind conditions and extended voyage durations are particularly sensitive to uncertainty. Taskar et al. (2023) employed a speed optimization algorithm to reduce fuel consumption up to 6% for a voyage and concluded that speed optimization helps save fuels in heavy weather conditions.

Some studies combined other factors such as cargo volume, ship scheduling, and fleet sizing with shipping route, speed, and bunkering to reduce emissions. For instance, Xia et al. (2021) investigated an innovative emission reduction strategy involving ship scheduling and speed reduction (SSSR). Through practical experiments using real-world data, they found that the SSSR method can reduce ship emissions by 8.0% to 11.9% and improve traffic efficiency by 3.8% to 6.2%. Moradi et al. (2022) utilized a reinforcement learning algorithm to optimize shipping routes for reducing fuel consumption and CO2 emissions. Numerical experiments demonstrated that this approach can achieve fuel savings of up to 6.64%. Sun et al. (2022) proposed a comprehensive optimization model encompassing fleet size, sailing paths, speeds, and the reallocation of ship CO2 emission permits. They utilized the CPLEX solver to address this complex problem. Zhang et al. (2023) introduced a mathematical model that considers various environmental factors such as water speed, depth, and cargo volume to optimize the speed and energy efficiency of inland all-electric ships operating in battery-swapping mode. They employed the Differential Evolution with Neighborhood Search (NSDE) algorithm to determine the optimal sailing speed in each segment, resulting in significant reductions in overall operational expenses.

While numerous studies have explored the optimization of route, speed, and bunkering at loading or unloading ports for shipping lines with conventional-fueled ships, no study has incorporated these decisions into the operation of alternative-fueled ships, such as LNG-fueled ships. Given the limited availability of ports for bunkering LNG, it becomes essential to jointly optimize the sailing route, sailing speeds, and bunkering at loading, unloading, or alternative bunker ports for LNG-fueled ships. Existing studies solely focus on the speed of each sailing leg and refueling at loading or unloading ports, without considering route adjustment and bunkering at alternative ports, making them unsuitable for the operations of LNG-fueled ships. To bridge this gap between research and practice, we have carried out this work.

3. Route, speed, and bunkering optimization for a tramp shipping line

3.1. Problem description

Consider a pre-determined tramp shipping line with multiple voyages for transporting a set of bulk cargoes. Each cargo is associated with a loading port and an unloading port, denoted by set $\mathcal{P}$ and $\mathcal{D}$, respectively. Each specific cargo cannot be shipped with other cargo together and has a latest loading and unloading start time ($n_i, i \in \mathcal{P} \cup \mathcal{D}$) along with a loading and unloading duration ($h_i, i \in \mathcal{P} \cup \mathcal{D}$). The shipping line is served by an LNG-fueled tramp ship anchored in port s, with a holding capacity (m) for the fuel tank and a fixed daily operation cost (c_{fix}). Some loading and unloading ports can bunker LNG, denoted by $\mathcal{P}_F$ and $\mathcal{D}_F$, respectively. Additionally, there are several alternative bunkering ports ($\mathcal{F}$) along the voyages, with bunkering prices varying among ports $c_i (i \in \mathcal{F} \cup \mathcal{P}_F \cup \mathcal{D}_F)$. The ship may detour to alternative ports for bunkering during voyages, particularly when some loading or discharging ports cannot bunker LNG.

The shipping company determines bunkering ports and volumes, the sailing route, and sailing speeds ($v \in \mathcal{V}, knot$) to minimize total costs for the tramp shipping line. These costs include bunkering costs at each bunkering port, fluctuation in the monetary value of the initial bunker f_s and residual bunker f_e, and daily operating costs for the ship. The initial bunker and residual bunker refer specifically to the fuel volume carried by the ship when it departs from the first port and arrives at the last port, respectively. The monetary value of the corresponding bunker is calculated by multiplying the fuel volume by the price at the associated port. This strategy ensures bunkering primarily occurs at ports with lower fuel prices (Meng et al., 2015).

We make three assumptions for model development. First, two loading conditions, laden and ballast, are considered for the ship, and they exhibit variations in fuel consumption at the same speed. Second, the fuel consumption per nautical mile (nmi) for the ship at a specific speed (v knots) in the laden or ballast condition is pre-determined. Third, shipping companies hedge against the volatility of LNG prices in the upcoming months by entering into medium-term contracts with bunkering ports.

All parameters and variables necessary for model development are listed as follows.

Set:

- $\mathcal{P}$: Set of loading ports;
- $\mathcal{D}$: Set of unloading ports;
- $\mathcal{F}$: Set of alternative bunkering ports, $\mathcal{F} \cap \{\mathcal{P} \cup \mathcal{D}\} = \emptyset$;
- $\mathcal{P}_F/\mathcal{D}_F$: Set of loading/unloading ports which can bunker LNG;
- $\mathcal{V}$: Set of alternative speeds;
- $\mathcal{N}$: Set of all ports, $\mathcal{N} = \{s\} \cup \mathcal{P} \cup \mathcal{D} \cup \mathcal{F}$.

Parameters:

- δ_v: Fuel consumption per nautical mile for the ship sailing at speed v (knot) in laden condition;
- δ'_v: Fuel consumption per nautical mile for the ship sailing at speed v (knot) in ballast condition;
- n_i: Latest call time for port $i, i \in \mathcal{P} \cup \mathcal{D}$;
- m: Holding capacity (mt) for the fuel tank of the ship;
- $\overline{m}$: Minimum residual fuel volume (mt) when calling a port;
- M: An extremely large constant;
- c_i: Bunkering price at port $i, i \in \mathcal{F} \cup \mathcal{P}_F \cup \mathcal{D}_F$;
- c_{fix}: Operating cost per day for the ship;
- f_s: Initial fuel volume (mt) when the ship departs from the first port;
- D_i: The unloading port associated with loading port $i, i \in \mathcal{P}$;
- s_i: Bunkering speed (mt) at port $i, i \in \mathcal{F} \cup \mathcal{P}_F \cup \mathcal{D}_F$;
- d_{ij}: Nautical miles between ports i and j, $\forall i, j \in \mathcal{N}$;
- t_{ij}^v: Sailing time (hours) from port i to port j with speed v (knot);
- h_i: Port time at port i, $i \in \mathcal{P} \cup \mathcal{D}$.

Decision Variables:

- $x_{ij}^v \in \{0, 1\}$: Whether or not the ship sails from port i to port j with speed v;
- $f_i \geq 0$: Amount of the residual fuel when reaching port i;
- $b_i \geq 0$: Amount of LNG refueled at port $i, i \in \mathcal{F} \cup \mathcal{P}_F \cup \mathcal{D}_F$;

- $a_i \geq 0$: Arrival time at port $i, i \in \mathcal{N}$;
- $\beta_i \in \{0, 1\}$: Whether or not sails to an alternative bunkering port after calling the loading port $i, i \in \mathcal{P}$;
- $\Delta \geq 0$: Total voyage time (day) for the shipping line.

3.2. Arc-based mixed-integer linear programming model

With the above definitions and notations, we can formulate this problem as an arc-based MILP model.

$$\min \sum_{i \in \mathcal{F} \cup \mathcal{P}_F} c_i b_i + c_s f_s - c_e f_e + c_{fix} \Delta \tag{1}$$

$$\sum_{v \in \mathcal{V}} x^v_{iD_i} + \beta_i = 1, \forall i \in \mathcal{P} \tag{2}$$

$$\sum_{j \in \mathcal{F}} \sum_{v \in \mathcal{V}} x^v_{ij} + \sum_{j \in \mathcal{F}} \sum_{v \in \mathcal{V}} x^v_{jD_i} = 2\beta_i, \forall i \in \mathcal{P} \tag{3}$$

$$\sum_{j \in \mathcal{N}} \sum_{v \in \mathcal{V}} x^v_{ij} = \sum_{j \in \mathcal{N}} \sum_{v \in \mathcal{V}} x^v_{ji}, \forall i \in \mathcal{N} \tag{4}$$

$$f_j \geq f_i + b_i - \sum_{v \in \mathcal{V}} d_{ij} \delta_v x^v_{ij} - M \left(1 - \sum_{v \in \mathcal{V}} x^v_{ij}\right), \forall i \in \mathcal{P} \text{ or } j \in \mathcal{D} \tag{5}$$

$$f_j \leq f_i + b_i - \sum_{v \in \mathcal{V}} d_{ij} \delta_v x^v_{ij} + M \left(1 - \sum_{v \in \mathcal{V}} x^v_{ij}\right), \forall i \in \mathcal{P} \text{ or } j \in \mathcal{D} \tag{6}$$

$$f_j \geq f_i + b_i - \sum_{v \in \mathcal{V}} d_{ij} \delta'_v x^v_{ij} - M \left(1 - \sum_{v \in \mathcal{V}} x^v_{ij}\right), \forall i \in \mathcal{N} \setminus \mathcal{P}, \forall j \in \mathcal{N} \setminus \mathcal{D} \tag{7}$$

$$f_j \leq f_i + b_i - \sum_{v \in \mathcal{V}} d_{ij} \delta'_v x^v_{ij} + M \left(1 - \sum_{v \in \mathcal{V}} x^v_{ij}\right), \forall i \in \mathcal{N} \setminus \mathcal{P}, \forall j \in \mathcal{N} \setminus \mathcal{D} \tag{8}$$

$$f_i + b_i \leq m, \forall i \in \mathcal{N} \tag{9}$$

$$f_i \geq \overline{m}, \forall i \in \mathcal{N} \tag{10}$$

$$a_j \geq a_i + h_i + \frac{b_i}{s_i} + \sum_{v \in \mathcal{V}} t^v_{ij} x^v_{ij} - M(1 - \sum_{v \in \mathcal{V}} x^v_{ij}), \forall i, j \in \mathcal{N} \tag{11}$$

$$a_i \leq n_i, \forall i \in \mathcal{P} \cup \mathcal{D} \tag{12}$$

$$\Delta \geq (a_e - a_s)/24 \tag{13}$$

The objective function (1) minimizes total costs, including bunker costs at each bunkering port, the difference in the monetary value between the initial bunker and the residual bunker, and daily operation costs throughout entire voyages for the ship. Constraints (2) impose that the ship either proceeds to its corresponding unloading port or an alternative bunker port for refueling, after loading cargo at port i. Constraints (3) enforce that if the ship sails to an alternative bunker port for refueling after loading cargo at port i, it must sail to the corresponding unloading port to unload cargo after completing the fuel refueling. Constraints (4) ensure that the inflow and outflow of the ship at node i are conserved. Constraints (5) and (6) specify the amount of residual fuel upon arrival at port j if the ship sails from port i to port j in the laden condition. Constraints (7) and (8) denote the amount of residual bunker upon arrival at port j if the ship sails from port i to port j in ballast condition. Constraints (9) ensure that the sum of the remaining fuel volume at port i and the fuel refueled at port i is less than the holding capacity of the fuel tank. Constraints (10) stipulate that the residual bunker at port i should be greater than the minimum fuel volume. Constraints (11) specify the time of call at the port. Constraint (12) restricts the call time to be less than the latest call time at the corresponding port. Constraint (13) indicates the total sailing time of the entire route.

3.3. Leg-based MILP model

The arc-based model can be solved directly by solvers like CPLEX or GUROBI. However, the decision space of this model is large due to the presence of numerous big-M constraints, preventing solvers from obtaining optimal solutions within a practical time limit. There are two common approaches to dealing with this situation. One is to design customized exact algorithms such as Branch-and-Price (Barnhart et al., 1998) or heuristic algorithms such as Variable Neighborhood Search (Mladenović and Hansen, 1997; Hansen and Mladenović, 2001) to solve the problem. Another approach is to build a more efficient mathematical formulation based on problem characteristics. For this problem, although the ship may take detours to alternative bunker ports for bunkering during voyages, the visit sequence for loading and unloading ports of the shipping line is known or can be determined. This allows us to model a 'leg-based' formulation, where each voyage from a loading (unloading) port to the next unloading (loading) port is defined as a 'leg'.

To provide a precise definition of this model, several terms need clarification: route, leg option, and stretch. The meanings of these terms are analogous to Fagerholt et al. (2015):

- *Route*: As shown in Fig. 4(a), route represents a shipping line with a pre-determined sequence of port calls, incorporating loading and unloading ports, but excluding alternative bunkering ports.
- *Leg*: Leg denotes the voyage between two adjacent loading and unloading ports along the route. As depicted in Fig. 4(a), there are three legs. For leg 2, there are two leg options, as shown in Figs. 4(b) and 4(c), respectively. Option 1 is the path from unloading port 1 to loading port 2, while option 2 makes a detour to call LNG bunkering port 1.
- *Stretches*: As shown in 4(c), option 2 comprises two stretches, with the first stretch sailing from unloading port 1 to bunkering port 1 and the second stretch sailing from bunkering port 1 to loading port 2. We assume that there is at most one alternative bunkering port for each leg. As such, each leg option has at most two stretches.

Given batches of cargo and the associated loading and unloading ports, the route for transporting them and the associated legs are straightforward. With these predetermined legs and alternative bunker ports along the route, it is possible to enumerate the options for each leg. Based on the route, legs, and options, the original problem can be reframed as selecting an option for each leg and identifying the speed and bunker decision for each chosen option. As a result, we formulate the original model as a leg-based model. The necessary notations for developing the leg-based model are listed as follows.

Set:

- $\mathcal{L}$: Set of sailing legs for the tramp ship;
- $\mathcal{L}_{BA}$: Set of sailing legs in ballast condition;
- $\mathcal{L}_{LA}$: Set of sailing legs in laden condition;
- $\mathcal{O}_l$: Set of options for leg l;
- $\mathcal{O}'_l$: Set of options with the bunkering ability at the first port of leg l;
- $\mathcal{O}''_l$: Set of options with the detour bunkering ability at an alternative port of leg l;
- $\mathcal{O}^s_l$: Set of stretches for option o of leg l.

Parameters:

- n_l: Latest call time for the last port on leg l;
- t^{sv}_{lo}: Sailing time for option o of leg l at speed v (knot);
- d^s_{lo}: Nautical miles of stretch s for option o of leg l;
- c^o_l: Bunker price ($/mt) for option o of leg l;
- s^o_l: Bunker speed (mt/hour) for option o of leg l;
- h^o_l: Port time (hour) for option o of leg l.

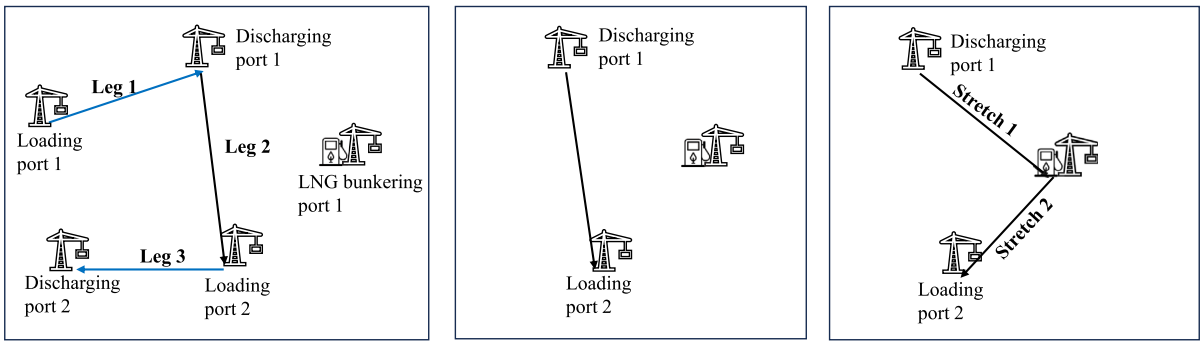

(a) Route with three legs (b) Option 1 with one stretch for leg 2 (c) Option 2 with two stretches for leg 2

Fig. 4. An illustrative example of the shipping route, leg, leg option, and stretch.

Decision Variables:

- $x_{lo}^{sv} \in \{0,1\}$: Whether the ship sails at speed v on stretch s for option o of leg l;
- $f_l \geq 0$: Remaining fuel when leg l is completed;
- $b_l^o \geq 0$: Bunker volume for option o of leg l;
- $a_l \geq 0$: Completion time for leg l;
- $\Delta \geq 0$: Total sailing time (day).

$$\min \sum_{l\in\mathcal{L}} \sum_{o\in\mathcal{O}_l} c_l^o b_l^o + c_s f_0 - c_e f_{|\mathcal{L}|} + c_{fix}\Delta \tag{14}$$

$$\sum_{o\in\mathcal{O}_l} \sum_{v\in\mathcal{V}} x_{lo}^{1v} = 1, \forall l \in \mathcal{L} \tag{15}$$

$$\sum_{v\in\mathcal{V}} x_{lo}^{1v} = \sum_{v\in\mathcal{V}} x_{lo}^{2v}, \forall l \in \mathcal{L}, \forall o \in \mathcal{O}_l'' \tag{16}$$

$$f_l = f_{l-1} + \sum_{o\in\mathcal{O}_l} b_l^o - \sum_{o\in\mathcal{O}_l} \sum_{s\in\mathcal{O}_l^s} \sum_{v\in\mathcal{V}} d_{lo}^s \delta_v x_{lo}^{sv}, \forall l \in \mathcal{L}_{LA}, \forall l-1 \in \mathcal{L} \tag{17}$$

$$f_l = f_{l-1} + \sum_{o\in\mathcal{O}_l} b_l^o - \sum_{o\in\mathcal{O}_l} \sum_{s\in\mathcal{O}_l^s} \sum_{v\in\mathcal{V}} d_{lo}^s \delta_v' x_{lo}^{sv}, \forall l \in \mathcal{L}_{BA}, \forall l-1 \in \mathcal{L} \tag{18}$$

$$b_l^o \leq m \sum_{v\in\mathcal{V}} x_{lo}^{1v}, \forall l \in \mathcal{L}, \forall o \in \mathcal{O}_l \tag{19}$$

$$f_{l-1} + \sum_{o\in\mathcal{O}_l'} b_l^o \leq m, \forall l \in \mathcal{L} \tag{20}$$

$$f_{l-1} + \sum_{o\in\mathcal{O}_l''} b_l^o - \sum_{o\in\mathcal{O}_l''} \sum_{v\in\mathcal{V}} d_{lo}^1 \delta_v x_{lo}^{sv} \leq m, \forall l \in \mathcal{L}_{LA} \tag{21}$$

$$f_{l-1} + \sum_{o\in\mathcal{O}_l''} b_l^o - \sum_{o\in\mathcal{O}_l''} \sum_{v\in\mathcal{V}} d_{lo}^1 \delta_v' x_{lo}^{sv} \leq m, \forall l \in \mathcal{L}_{BA} \tag{22}$$

$$f_l \geq \overline{m}, \forall l \in \mathcal{L} \tag{23}$$

$$f_{l-1} - \sum_{o\in\mathcal{O}_l''} \sum_{v\in\mathcal{V}} d_{lo}^1 \delta_v x_{lo}^{sv} \geq \overline{m}, \forall l-1 \in \mathcal{L}_{LA} \tag{24}$$

$$f_{l-1} - \sum_{o\in\mathcal{O}_l''} \sum_{v\in\mathcal{V}} d_{lo}^1 \delta_v' x_{lo}^{sv} \geq \overline{m}, \forall l-1 \in \mathcal{L}_{BA} \tag{25}$$

$$a_l \geq a_{l-1} + \sum_{o\in\mathcal{O}_l} \sum_{s\in\mathcal{O}_l^s} \sum_{v\in\mathcal{V}} t_{lo}^{sv} x_{lo}^{sv} + \sum_{o\in\mathcal{O}_l'} \sum_{v\in\mathcal{V}} h_l^o x_{lo}^{1v} + \frac{b_l^o}{s_l^o}, \forall l, l-1 \in \mathcal{L} \tag{26}$$

$$a_l \leq n_l, \forall l \in \mathcal{L} \tag{27}$$

$$\Delta \geq (a_{|\mathcal{L}|} - a_0)/24 \tag{28}$$

Objective function (14) minimizes total costs, including bunker costs at each bunkering port, the difference in the monetary value between the initial bunker and the residual bunker, and daily operation costs throughout the entire route for the ship. Constraints (15) ensure that each leg must be fulfilled. Constraints (16) impose that each stretch of option o must be fulfilled if option o of leg l is selected. Constraints (17) identify the amount of remaining fuel upon the completion of the voyage of leg l if the ship sails through leg l in laden condition. Constraints (18) identify the amount of remaining fuel upon the completion of the voyage of leg l if the ship sails on leg l in ballast condition. Constraints (19) enforce that option o of leg l must be fulfilled if the ship bunkers at the bunkering port of option o of leg l. Constraints (20)–(22) ensure that the remaining amount of fuel on the leg l plus the bunker volume is less than the holding capacity of the fuel tank. Constraints (23)–(25) indicate that the amount of fuel remaining after the completion of a leg should be greater than the minimum fuel volume. Constraints (26) determine the call time at port j. Constraints (27) restrict the call time to be less than the latest call time at the corresponding port. Constraint (28) indicates the total sailing time of the entire shipping line.

Note that these two models are also applicable to tramp shipping lines utilizing alternative fuels, such as methanol. Given the commonalities in the operation of alternative-fueled ships, specifically the scarcity of bunkering ports and thus the necessity to detour other ports for refueling beyond standard loading and unloading ports, joint decisions on routing, speeds, and bunkering have become indispensable. These factors are built into the models, making them appropriate for application on tramp shipping lines powered by various alternative fuels.

4. Case study

In this section, we initially assess the performance of the arc-based and leg-based formulations. Subsequently, a tramp shipping route with three voyages is utilized for numerical experiments. The formulations are solved using CPLEX 12.8 and implemented in C++.

4.1. Experimental setting

Consider an LNG-fueled tramp ship with a loading capacity of 200,000 tons, equipped with an LNG-fuel tank that can hold up to 6000 metric tons. We set the safe fuel volume at 500 mt. The ship carries 3000 mt of LNG fuel when departing from the port of Jingtang. The ship's daily operation cost is $5000. The fuel consumption per hour under laden and ballast conditions at speed v is given by $0.6826 \times v^{1.7984}/24$ and $0.0139 \times v^{3.1284}/24$, respectively. The service speed of the ship is 15 knots. We set the minimum speed of the ship to 8 knots, namely, the interval of the sailing speed is [8.0, 15.0]. The ship is scheduled to depart from Jingtang port to undertake a tramp shipping line encompassing three transportation tasks. The corresponding loading and unloading ports for these tasks are Ningbo-Singapore, Hedland-Long Beach, and San Antonio (CL)–Jingtang. The latest times of call at loading and unloading ports are shown in Table 1.

Table 1
Loading and unloading ports.

Ports	Ningbo	Singapore	Hedland	Long beach	San Antonio (CL)	Jingtang
Latest time of call (hour)	64	480	720	1440	3000	3120
Call purpose	Load	Unload	Load	Unload	Load	Unload
Port time (hour)	12	24	12	24	12	24

Fig. 5. The tramp shipping route (Jingtang–Ningbo–Singapore–Hedland–Long Beach–San Antonio (CL)–Jingtang) and eight alternative bunker ports.

Among the five loading and unloading ports, only Ningbo, Singapore, and Long Beach have LNG bunker capabilities. In addition, there are eight alternative LNG bunker ports: Shanghai, Shenzhen, Balawan, Pengerang, Dampier, Vancouver, Tacoma, and Pananam City, as illustrated in Fig. 5. Therefore, the original route can make some detours to bunker at these alternative bunkering ports. For instance, the sailing leg from Jingtang port to Singapore port can bunker LNG fuel at Shanghai, Ningbo, or Shenzhen port. The route comprises six legs: Jingtang–Ningbo, Ningbo–Singapore, Singapore–Hedland, Hedland–Long Beach, Long Beach–San Antonio, and San Antonio (CL)–Jingtang. The bunkering speed of all bunker ports is 1000 mt/hour, and the fuel price of the ports ranges from $600-$700 per mt, randomly generated.

4.2. Computational performances of arc-based and leg-based models

Given the route and the alternative bunkering ports, a set of test instances is generated to assess the computational performance of two mathematical models, with the results summarized in Table 2. In column (1) of Table 2, "T" denotes the number of transportation tasks, "O" is the number of alternative bunker ports, and "B" represents the number of loading and unloading ports that can bunker LNG. The "Obj" values in columns (2) and (5) indicate the objective values of the solutions identified by the arc-based model and the leg-based model, respectively. "Gap" in columns (3) and (6) signifies the difference between the objective value of the solution and the lower bound of the two models, respectively. The term "Time" in columns (4) and (7) denotes the computation time for the two models, respectively. Columns (8) and (9) are the percentage improvement in solution quality and computation time of the leg-based model compared to the arc-based model, respectively. The computational results reveal that the arc-based model exhibits weak computation performance, with optimality gaps larger than 80% for most instances after two hours of computing. In contrast, the leg-based model can identify optimal solutions for all instances within two seconds, highlighting its superior computational performance.

4.3. Impacts of bunkering at alternative ports

To assess the impact of bunkering at alternative ports on operating costs and fuel consumption, compared to refueling at ports of loading and unloading, two sets of experiments are conducted. The first set of experiments explores the impact of varying numbers of alternative refueling ports, while the second set of experiments examines the influence of different fuel prices among ports.

The first set of experiments consists of four cases. In case 1, the ship can bunker at only three loading and unloading ports. In cases 2, 3, and 4, the ship can bunker at eight, five, and two alternative bunkering ports, respectively. The details of bunkering ports for each case are presented in Table 3, with the bunkering price set at $ 600 per mt for all ports. The experimental results are presented in Table 4. These computation results reveal that the differences in operating costs and fuel consumption between the two bunkering modes are negligible when there are enough alternative bunkering ports, as in Case 2. Specifically, compared to Case 1, the total cost of Case 2 increases by only 0.13%, the amount of fuel refueled increases by only 0.48%, and fuel consumption increases by only 0.18%. However, when there are fewer alternative bunkering ports, as in Case 4, differences between the two bunkering modes emerge. Compared to Case 1, Case 4 exhibits an increase in total cost, bunker volume, and fuel consumption by 3.03%, 10.51%, and 3.87%, respectively. This is because when there are more alternative bunkering ports, bunker volume at alternative ports leads to less route deviation, resulting in less deviation in sailing distances and speeds between bunker modes.

The second set of experiments examines variations in total costs, bunker volume, and fuel consumption between the two bunkering modes at different fuel prices among ports. Starting with a base fuel price of $600 per mt, the upper limit of the price variation is incrementally set at 1%, 2%, 3%, …, up to 30%, resulting in a total

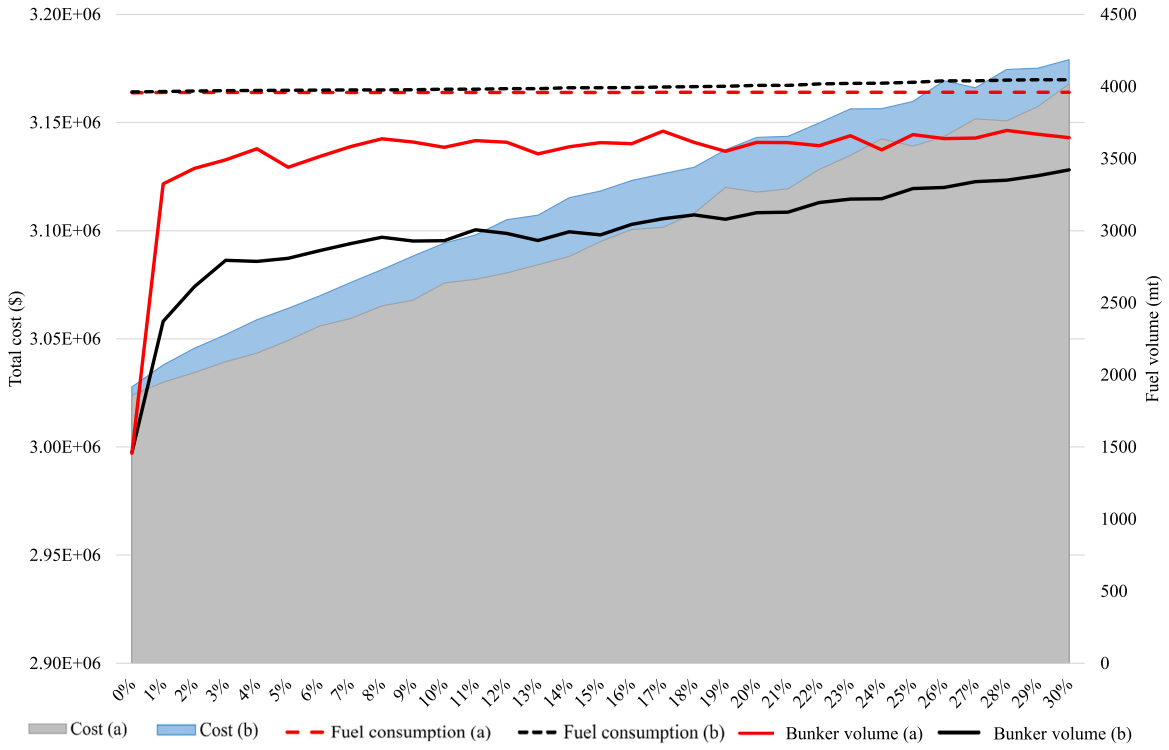

Fig. 6. The impact of bunkering at alternative LNG-fuel ports under different fuel price variations.

Table 2
Computational performances for two models.

Instances	Arc-based model			Leg-based model			Improvement	
	Obj ($)	Gap (%)	Time (%)	Obj ($)	Gap (%)	Time (%)	Gap (%)	Time (%)
(1)	(2)	(3)	(4)	(5)	(6)	(7)	(8)	(9)
T1O1B1	1814870	0.00	0.14	1814870	0.00	0.03	0.00	78.57
T2O1B1	2 961 420	0.00	1.45	2 961 420	0.00	0.08	0.00	94.48
T2O2B1	3 010 650	81.46	7200.08	3 010 650	0.00	0.16	0.00	100.00
T2O2B2	2 952 870	0.00	779.23	2 952 870	0.00	1.69	0.00	99.78
T2O3B1	3 085 630	0.00	1107.48	3 085 630	0.00	0.61	0.00	99.94
T2O3B2	2 996 940	0.00	426.75	2 996 940	0.00	0.13	0.00	99.97
T3O2B1	3 295 370	0.00	4.50	3 295 370	0.00	0.92	0.00	79.56
T3O2B2	3 300 370	0.00	3.97	3 300 370	0.00	0.88	0.00	77.83
T3O3B1	3 400 550	82.47	7201.20	3 400 420	0.00	0.34	0.00	100.00
T3O3B2	3 212 690	103.62	7200.41	3 212 690	0.00	0.48	0.00	99.99
T3O4B2	3 284 680	101.34	7201.83	3 284 680	0.00	0.31	0.00	100.00
T3O5B2	3 215 910	138.59	7200.17	3 200 330	0.00	1.41	0.48	99.98
Average	**3 044 329**	**38.96**	**3193.93**	**3 043 020**	**0.00**	**0.59**	**0.04**	**94.18**

*(8) = [(2) − (5)]/(2) × 100%; (9) = [(2) − (7)]/(2) × 100%.

Table 3
Cases with different bunkering ports.

Cases	Alternative bunker ports
Case 1	1. Ningbo, 2. Singapore, and 3. Long Beach
Case 2	1. Shanghai, 2. Shenzhen, 3. Belawan, 4. Pengerang, 5. Dampier, 6. Tacoma, 7. Vancouver, and 8. Panama City
Case 3	1. Shanghai, 2. Belawan, 3. Dampier, 4. Vancouver, and 5. Panama City
Case 4	1. Belawan and 2. Panama City

of 31 scenarios. For instance, if the upper boundary of fuel price variation is set at 3%, it implies that fuel prices in these ports are randomly generated within the interval [600, 618]. To mitigate randomness, one hundred experiments, with prices randomly generated within the corresponding price interval, are conducted in each scenario. The corresponding average values of total costs, bunker volume, and fuel consumption of the two bunker modes with different bunkering ports are depicted in Fig. 6, where (a) and (b) represent bunkering at loading/unloading ports and bunkering at alternative bunkering ports, respectively. For instance, "Cost (a)" denotes the total costs for bunkering at loading/unloading ports, while "Cost (b)" implies the total costs for bunkering at alternative ports. As observed from the figure, regardless of oil price fluctuations, bunkering at alternative ports leads to an approximate 0.6% increase in total costs, a 0.99% increase in fuel consumption, and an 18% decrease in bunker volume. In conclusion, operating costs exhibit fluctuations with fuel price variations, increasing as fuel price fluctuations intensify, while these fluctuations have a comparatively lesser impact on fuel consumption and bunker volume. It is essential to note that the total voyage time remains constant at 130 days under different scenarios due to the restriction of the latest call time at each loading/unloading port.

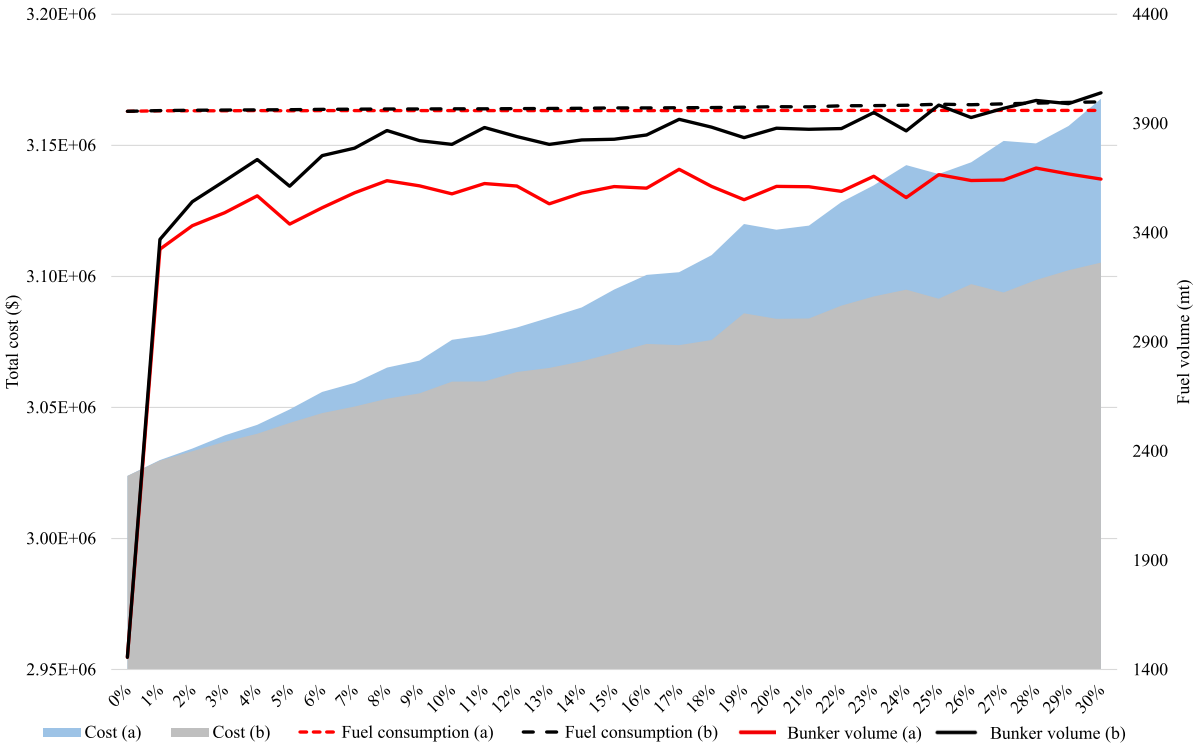

Fig. 7. The impact of bunkering with alternative LNG-fuel ports under different fuel price variations.

Table 4
Impacts of bunkering with detour.

Cases	Total cost ($)	Voyage time (day)	Shipping line	Sailing speed (knot)	Bunkering (mt)	Fuel consumption (mt)
Case 1	3 023 840	130	Jingtang–Ningbo–Singapore –Hedland–Long Beach –San Antonio (CL)–Jingtang	11.4–9.0–9.1 –9.2–9.2–9.2	Long Beach: 1456	3956
Case 2	3 027 670	130	Jingtang–Ningbo–Shenzhen –Singapore–Hedland–Long Beach –San Antonio (CL)–Jingtang	11.4–9.3–9.2– 9.2–9.2–9.1–9.2	Shenzhen: 1463	3963
Case 3	3 040 690	130	Jingtang–Ningbo–Singapore –Dampier–Hedland–Long Beach –San Antonio (CL)–Jingtang	11.4–9.3–9.3–9.1 –9.3–9.1–9.2	Dampier: 1485	3985
Case 4	3 115 350	130	Jingtang–Ningbo–Singapore –Belawan–Hedland–Long Beach –San Antonio (CL)–Jingtang	11.4–9.6–9.6–9.4 –9.7–9.2–9.3	Belawan: 1609	4109

4.4. Bunkering at alternative ports and loading/unloading ports with bunker capability

To analyze the impact of the bunker mode that allows fuel refueling at both alternative bunker ports and loading/unloading ports with bunker capability, compared to the mode allowing fuel refueling only at loading/unloading ports, experiments are conducted under different fuel price fluctuations to analyze changes in total costs, bunker volume, and fuel consumption. We also use $600 per mt as the base fuel price and consider price fluctuations of 1%, 2%, …,30%, resulting in 31 scenarios in total. To mitigate randomness, one hundred experiments are conducted in each scenario. The corresponding average values of total costs, bunker volume, and fuel consumption are shown in Fig. 7, where (a) denotes the case of bunkering at loading/unloading ports, and (b) denotes the case in which the fuel can be bunkered at loading/unloading ports with LNG bunker capability or alternative bunkering ports. The results demonstrate that bunkering with alternative ports is effective in reducing total shipping costs as fuel price volatility increases since it provides options to bunker fuel at ports with cheaper bunker prices. This explains why overall bunker volume is higher than bunkering at loading/unloading ports only. The bunker mode with alternative bunkering ports reduces the total cost by 2% when the price fluctuation is 30%. Consistent with the experimental results in the previous section, price volatility has a small effect on fuel consumption and refueling.

5. Conclusion

Alternative-fueled ships are helpful in effectively reducing emissions and pollution. However, many ports lack the capability to bunker alternative fuels such as LNG and methanol. As a result, these ships may detour to alternative-fueled ships to refuel at bunkering ports other than their loading and unloading ports, introducing new operational challenges.

In this paper, we address a joint optimization problem involving decisions on the shipping route, sailing speeds, and fuel refueling strategy for LNG-fueled tramp ships. We establish an arc-based mixed-integer programming model intending to minimize total operating costs. Additionally, we formulate a leg-based mathematical model tailored to the problem characteristics, capable of obtaining optimal solutions within

two seconds for practical instances. To validate the correctness and effectiveness of the models and explore the operational differences between LNG-fueled and traditional ships, we conduct case studies based on a tramp shipping line. Experimental results demonstrate that, by factoring in speed and fuel bunkering decisions, bunkering at alternative ports does not impact voyage time and can effectively reduce total operational costs, particularly when there is a substantial difference in fuel prices between ports.

For future work, robust optimization or stochastic programming methods can be applied to model bunkering price volatilities among ports. Additionally, exploring the joint optimization of the shipping route, sailing speed, bunkering strategy, and fleet deployment for liner shipping with alternative-fueled ships would be beneficial. Furthermore, it is worthwhile to investigate the shipping line operations of dual-fuel powered ships, capable of utilizing two types of fuels to reduce fuel costs, which presents a more intricate decision-making challenge due to the complexities associated with fuel-switching. Lastly, it is a promising research topic to consider the effect of navigational weather and environment on fuel consumption in the joint optimization of sailing routes, speeds, and bunkering (Zis et al., 2020).

CRediT authorship contribution statement

Ping He: Writing – original draft, Software, Methodology, Conceptualization. **Jian Gang Jin:** Writing – review & editing, Supervision, Methodology, Funding acquisition, Conceptualization. **Wei Pan:** Writing – review & editing, Conceptualization. **Jianghang Chen:** Writing – review & editing, Conceptualization.

Declaration of competing interest

The authors declare that they have no known competing financial interests or personal relationships that could have appeared to influence the work reported in this paper.

Data availability

Data will be made available on request.

Acknowledgment

This work is supported by the National Natural Science Foundation of China [Grant 72122014] and the Research Development Fund [RDF-20-02-13] in XJTLU.

References

Balcombe, P., Staffell, I., Kerdan, I.G., Speirs, J.F., Brandon, N.P., Hawkes, A.D., 2021. How can LNG-fuelled ships meet decarbonisation targets? An environmental and economic analysis. Energy 227, 120462.

Barnhart, C., Johnson, E.L., Nemhauser, G.L., Savelsbergh, M.W.P., Vance, P.H., 1998. Branch-and-price: Column generation for solving huge integer programs. Oper. Res. 46 (3), 316–329.

Bayraktar, M., Yuksel, O., 2023. A scenario-based assessment of the energy efficiency existing ship index (EEXI) and carbon intensity indicator (CII) regulations. Ocean Eng. 278, 114295.

Deniz, C., Zincir, B., 2016. Environmental and economical assessment of alternative marine fuels. J. Clean. Prod. 113, 438–449.

Fagerholt, K., Gausel, N.T., Rakke, J.G., Psaraftis, H.N., 2015. Maritime routing and speed optimization with emission control areas. Transp. Res. C 52, 57–73.

Fagerholt, K., Laporte, G., Norstad, I., 2010. Reducing fuel emissions by optimizing speed on shipping routes. J. Oper. Res. Soc. 61, 523–529.

Hansen, P., Mladenović, N., 2001. Variable neighborhood search: Principles and applications. European J. Oper. Res. 130 (3), 449–467.

Hansson, J., Månsson, S., Brynolf, S., Grahn, M., 2019. Alternative marine fuels: Prospects based on multi-criteria decision analysis involving Swedish stakeholders. Biomass Bioenergy 126, 159–173.

Lindstad, E., Polić, D., Rialland, A., Sandaas, I., Stokke, T., 2022. Decarbonizing bulk shipping combining ship design and alternative power. Ocean Eng. 266, 112798.

Mason, J., Larkin, A., Bullock, S., van der Kolk, N., Broderick, J.F., 2023a. Quantifying voyage optimisation with wind propulsion for short-term CO2 mitigation in shipping. Ocean Eng. 289, 116065.

Mason, J., Larkin, A., Gallego-Schmid, A., 2023b. Mitigating stochastic uncertainty from weather routing for ships with wind propulsion. Ocean Eng. 281, 114674.

Meng, Q., Wang, S., Lee, C.Y., 2015. A tailored branch-and-price approach for a joint tramp ship routing and bunkering problem. Transp. Res. B 72, 1–19.

Mladenović, N., Hansen, P., 1997. Variable neighborhood search. Comput. Oper. Res. 24 (11), 1097–1100.

Moradi, M.H., Brutsche, M., Wenig, M., Wagner, U., Koch, T., 2022. Marine route optimization using reinforcement learning approach to reduce fuel consumption and consequently minimize CO2 emissions. Ocean Eng. 259, 111882.

Norstad, I., Fagerholt, K., Laporte, G., 2011. Tramp ship routing and scheduling with speed optimization. Transp. Res. C 19, 853–865.

Ren, J., Liang, H., 2017. Measuring the sustainability of marine fuels: A fuzzy group multi-criteria decision making approach. Transp. Res. D 54, 12–29.

Sun, Y., Zheng, J., Han, J., Liu, H., Zhao, Z., 2022. Allocation and reallocation of ship emission permits for liner shipping. Ocean Eng. 266, 112976.

Taskar, B., Sasmal, K., Yiew, L.J., 2023. A case study for the assessment of fuel savings using speed optimization. Ocean Eng. 274, 113990.

Wang, K., Li, J., Huang, L., Ma, R., Jiang, X., Yuan, Y., Mwero, N.A., Negenborn, R.R., Sun, P., Yan, X., 2020. A novel method for joint optimization of the sailing route and speed considering multiple environmental factors for more energy efficient shipping. Ocean Eng. 216, 107591.

Wei, Z., Zhao, L., Zhang, X., Lv, W., 2022. Jointly optimizing ocean shipping routes and sailing speed while considering involuntary and voluntary speed loss. Ocean Eng. 245, 110460.

Xia, Z., Guo, Z., Wang, W., Jiang, Y., 2021. Joint optimization of ship scheduling and speed reduction: A new strategy considering high transport efficiency and low carbon of ships in port. Ocean Eng. 233, 109224.

Zhang, Y., Sun, L., Fan, T., Ma, F., Xiong, Y., 2023. Speed and energy optimization method for the inland all-electric ship in battery-swapping mode. Ocean Eng. 284, 115234.

Zhen, L., Wang, S., Zhuge, D., 2017. Dynamic programming for optimal ship refueling decision. Transp. Res. E 100, 63–74.

Zhen, L., Wang, S., Zhuge, D., 2020. Route and speed optimization for liner ships under emission control policies. Transp. Res. C 110, 330–345.

Zis, T.P., Psaraftis, H.N., Ding, L., 2020. Ship weather routing: A taxonomy and survey. Ocean Eng. 213, 107697.